Article

Antihyperglycemic Potential of Quercetin-3-glucoside Isolated from *Leucaena leucocephala* Seedpods via the SIRT1/AMPK/GLUT4 Signaling Cascade

Pranamika Sarma, Bhaswati Kashyap, Shalini Gurumayum, Srutishree Sarma, Paran Baruah, Deepsikha Swargiary, Abhipsa Saikia, Ramesh Ch. Deka, and Jagat C Borah*

Cite This: *ACS Omega* 2024, 9, 32429−32443

Read Online

ACCESS | Metrics & More | Article Recommendations | Supporting Information

ABSTRACT: *Leucaena leucocephala.* (Lam.) de Wit, a traditional medicinal plant, has been reported among the ethnic communities of Mexico, Indonesia, China, and India for the treatment of diabetes, obesity, and related complications. This study investigates the antihyperglycemic activity of the plant and its isolated active compound quercetin-3-glucoside. Further, bioactivity guided marker assisted development of an enriched bioactive fraction toward enhancing insulin sensitization was carried out. The enriched fraction was also found to contain 397.96 mg/g of quercetin-3-glucoside along with three other marker compounds, which were also isolated and identified. Quercetin-3-glucoside, out of the four isolated marker compounds from the plant, showed the most significant bioactivity when tested in palmitate-induced insulin-resistant C2C12 myotubes. The compound also showed significant upregulation of sirtuin1 (SIRT1) followed by enhancement of insulin-dependent signaling molecules SIRT1/AMPK/PGC1-α and GLUT4 translocation. Molecular dynamics studies showed the compound having stable interactions with the SIRT1 protein. SIRT1 upregulation has been associated with enhanced insulin sensitivity in skeletal muscle, increasing the glucose uptake by muscle cells. The prepared enriched fraction also modulated the SIRT1/AMPK/ GLUT4 pathway. The findings of the present study may find future application toward the development of botanical or phytopharmaceutical drugs from the traditionally important plant *L. leucocephala* against type II diabetes.
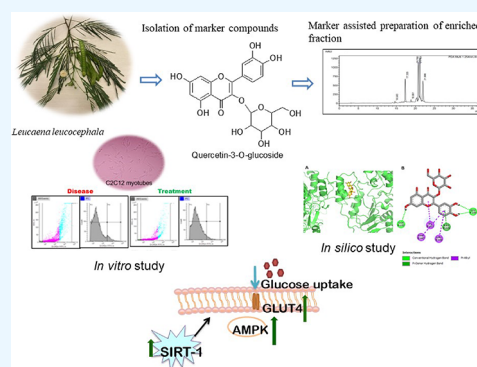
1. INTRODUCTION

Type II diabetes (T2D) is one of the major metabolic disorders, insulin resistance being one of the critical factors leading to the development of the condition. Studies have shown that elevated glucose and free fatty acid levels in diabetic condition cause disbalance in the delicate antioxidant defense mechanism of the body.[1] Mitochondrial reactive oxygen species (ROS) have been reported as one of the major events resulting in insulin resistance in skeletal muscle and adipose tissues. Skeletal muscles take up to 75% of circulating blood glucose, contributing to the glucose homeostasis in the body. The onset of insulin resistance condition reduces the glucose sensitivity of the cells, eventually leading to the pathogenesis of T2D.[2] Responding to the energy need of the body, ATP (adenosine triphosphate) is synthesized, with the major portion being generated in the mitochondria.[3] In normal physiological conditions, mitochondrial turnover takes place through a process called mitochondrial biogenesis. Recent evidence supports the involvement of 5′-adenosine mono-phosphate-activated protein kinase (AMPK) in the regulation of mitochondrial biogenesis. The peroxisome proliferator-activated receptor coactivator 1-alpha (PGC1-α) regulates the genes involved in the mitochondrial metabolism.[3] Mitochon-

dria are also one of the key cellular ROS generation sites. However, ROS overproduction negatively impacts the morphology and function of mitochondria.[4] Increased levels of free fatty acids (FFA) in the body can further exacerbate insulin resistance. Increased FFA and blood glucose levels upregulates the concentrations of tricarboxylic acid (TCA) cycle products acetyl coenzyme A and nicotinamide adenine dinucleotide, causing acetylation of the mitochondrial proteins.[5] In mammalian physiology, the nicotinamide adenine dinucleotide dependent enzyme sirtuin1 (SIRT1) is involved in the deacetylation process, thereby regulating insulin sensitivity. Increased glucose levels in the body decrease protein expressions related to SIRT1 in the process, increasing acetylation of the mitochondrial proteins.[5] Thus, targeting the upregulation of SIRT1 expressions and regulation of reactive
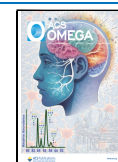
oxygen species in the body can serve as a potential therapeutic approach in enhancing insulin sensitivity and thereby treating type II diabetes.[6]

Leucaena leucocephala (Lam.) de Wit is a tropical shrub native to the southern Mexico and northern central America (Belize and Guatemala) but widely available in most of the tropics and subtropics including the Caribbean islands, southern and southeast Asian countries, Australia, African countries, and the Virgin islands of the USA.[7] Traditional usage of the different parts of the plant is found since the time of the Mayan civilization.[8] The plant is also reported as a traditional medicinal plant, and ethnomedicinal data from Mexico reports *L. leucocephala* raw seeds as a hypoglycemic agent.[9] In different parts of Indonesia, the plant seeds are also used for the treatment of diabetes mellitus.[10] In Chinese traditional medicine, the plant is known as "Chinese petai" and is used in swelling, diabetes, and kidney inflammation.[11] Ethnopharmacological uses of the plant are also available from different parts of the Indian subcontinent. The seeds are reported to be used as a hypoglycemic agent in folk medicine.[12] In Manipur, India, Meitei and Meitei-Pangal communities primarily use leaf decoction for the treatment of diabetes.[13] It is also used to treat pain and inflammation in traditional South African medicine.[14] However, bioactivity guided phytochemical analyses to identify the active antihyperglycemic constituents of the various extracts of the plant and studies on the underlying mechanism of action are scarce in the literature. The development of novel therapeutic interventions from the plant requires bioactivity guided identification of the active phytoconstituents responsible for its bioactivity. Further marker assisted standardization of a new chemically defined entity can open up new horizons in the medicinal use of the traditionally widely acclaimed plant *L. leucocephala*. This study thus aims to conduct a bioactivity guided investigation of antidiabetic fractions of *L. leucocephala* and identify the chemical constituents present in the active fraction responsible for the activity.

2. MATERIAL AND METHODS

2.1. Reagents and Chemicals. A triple quadruple mass spectrometer (Thermo Scientific Exactive Plus, Orbitrap) with ion source ESI (electron spray ionization) from Thermo Scientific was used for obtaining the mass spectra. A Shimadzu LC-20 AD high-performance liquid chromatography (HPLC) system fitted with a Prominence photodiode array (PDA) detector was used for all HPLC analyses and isolation of molecules. Discovery reversed phase (RP) C-18 analytical (Supelco, 5 μm, 250 × 4.6 mm) and semipreparative (Supelco 10 μm, 250 × 10 mm) HPLC columns were used for analytical and semipreparative HPLC respectively. All HPLC solvents used were gradient grade HPLC solvents from Merck. Silica gel (Merck, 100−200 mesh size) from Sigma-Aldrich was used for column chromatography. Normal-phase TLC (thin layer chromatography) plates precoated with silica gel (Merck) were used for thin layer chromatographic analysis. All solvents used for extraction and fractionation were of analytical grade. Sodium palmitate (cat. # P9767), bovine serum albumin (cat. # A-9647), insulin solution human (cat. # I972), Triton-X (cat. # T8787, 250 mL), α-dimethyl sulfoxide (D9418), 2′,7′-dichlorodihydrofluorescein diacetate (H$_2$DCFDA, cat. # D6883), *tert*-butyl hydroperoxide solution (TBHP), RIPA (radioimmunoprecipitation assay) buffer (cat. # R0278, 50 mL), acrylamide (cat. #A3553, 1 kg), bis-acrylamide (cat. #

M7279), Dulbecco's modified Eagle medium (DMEM, cat. # 12800017) high glucose (4.5 g/L), sodium bicarbonate (cat. # S5761), and sodium dodecyl sulfate (SDS) were purchased from Sigma- Aldrich. Fetal bovine serum (FBS, cat. # 16140071), trypsin (cat. # 25200072), antibiotic−antimycotic (cat. # 15240062), Dulbecco's phosphate-buffered saline (DPBS, cat. # 21300025), and 2-deoxy-2-[(7-nitro-2,1,3-benzoxadiazol-4-yl)amino]-D-glucose (2-NBDG, cat. # N13195) were from Invitrogen, India. Halt Protease and Phosphatase Inhibitor Cocktail (EDTA-free, 100×) was obtained from Thermo Scientific. Phenylmethylsulfonyl fluoride (PMSF) was from Roche, and glycine, tris base, and sodium chloride were purchased from Hi-Media. SDS (sodium dodecyl sulfate) and Tween 20 were from Merck, and nitrocellulose membrane 0.2 μm × 30 cm × 3.5 m (Biorad 1620112) and Precision Plus Dual Color Marker (1610374) were from Biorad. Anti-beta-actin antibody (AC-15) (HRP) was from Abchem (#ab49900), and AMPK-α antibody (#2532), phospho-AMPK alpha (Thr172) rabbit mab (#2535), antirabbit IgG HRP-linked antibody (#7074), and SIRT-1 (#9475S) were from Cell Signaling Technology. GLUT4 (#49533) was from Novus Biologicals. All other chemicals were purchased from Sigma, unless otherwise mentioned.

2.2. Plant Material. Mature unripe fruits of *Leucaena leucocephala* (Lam.) de Wit, commonly known as white lead tree, river tamarind, or ipil-ipil, were collected from the Kamrup metro district of Assam, North East India (26° 8′ 52.9548″ N and 91° 43′ 52.9572″ E) during the months of August and September 2020. The herbarium was prepared and deposited in the Department of Botany, Gauhati University, Assam, India, to obtain the accession no. GUBH20002. "The plant list" was used to quote the taxonomically accepted name of the plant.

2.3. Extraction and Fractionation. A 3.2 kg portion of dried powdered seeds of *L. leucocephala* was extracted using methanol as a solvent (4 L, 24 h × 3) at room temperature. The filtered extract was evaporated in a rotary evaporator to yield 250 g of crude extract. The evaporated crude extract was further lyophilized overnight to free it from all residual solvents. Fractionation of the crude extract was carried out by the liquid−liquid partition chromatography. Briefly, 130 g of the crude extract was suspended in the minimum volume of distilled water (150 mL) and fractionated in a separating funnel using hexane, ethyl acetate, and *n*-butanol. After rotary evaporation of the fractions, 19 g of the hexane fraction, 14 g of the ethyl acetate fraction (EAF), 32 g of the *n*-butanol fraction (BuF), and 35 g of the water fraction (WF) were obtained. The crude extract and all of the fractions were stored at −20 °C for future chemical investigation and evaluation of therapeutic potential.

2.4. Photometric DPPH Scavenging Assay. The crude extract and the ethyl acetate fraction, *n*-butanol fraction, and water fraction were subjected to a 2,2-diphenyl-1-picrylhydrazyl (DPPH) scavenging assay to assess their radical scavenging potential. A 1 mg/mL stock solution was prepared for each of the samples in methanol, and successive dilution was carried out to prepare test solutions of 10, 20, 50, 75, and 100 μg/mL concentrations. DPPH solution (270 μL, 0.2 mM) was added to each sample before incubating for 60 min in the dark. Ascorbic acid was used as a positive control, and DPPH with methanol served as a negative control. Absorbance was recorded at 517 nm. The half-maximal inhibitory concen-

tration (IC$_{50}$) was calculated from concentration vs % inhibition curves where the abscissa denotes the concentration of the extract and different fractions and the ordinate represents the average antioxidant activity calculated from three independent tests.

2.5. C2C12 Muscle Cell Culture. The C2C12 muscle cell line was procured from Sigma-Aldrich and cultured in a high glucose containing (4.5 g/L) Dulbecco's modified Eagle's medium (DMEM) enriched with 10% heat-inactivated fetal bovine serum (FBS) and 1% antibiotic and antimycotic mixture (containing 10,000 μg/mL of penicillin, 10,000 μg/mL of streptomycin, and 25 μg/mL of Gibco amphotericin B). The cells were incubated in a CO$_2$ incubator with 5% CO$_2$ at 37 °C. Once the cells were 90% confluent, the medium was changed from 10% FBS to 2% FBS to obtain myoblast differentiation to form mature myotubes.

2.6. Cell Viability Assay. A 3-(4,5-dimethylthiazol-2-yl)-2,5-diphenyltetrazolium bromide (MTT) was used to assess the cell viability of the plant sample. The cultured myotubes were treated with various concentrations of *L. leucocephala* crude extract and the fractions for 24 h. MTT crystals were dissolved in Dulbecco's phosphate-buffered saline of 7.4 pH to prepare a stock solution of 5 mg/mL. After that, 10 μL of the MTT solution (resulting in a final concentration of 0.5 mg/mL) was added, and the cells were incubated at 37 °C. After 4 h, the medium was replaced, and 100 μL of DMSO (dimethyl sulfoxide) was added to each well. Absorbance was measured at 570 nm by using a Biorad multiplate reader. Cell viability was expressed as percentage over control, and the following equation was used to calculate the cell viability:

$$\% \text{ Cell viability} = (As/Ac) \times 100$$

where As = absorbance of the test samples and Ac = absorbance of the control.

2.7. Preparation of the Free Fatty Acid (FFA) Solution. According to previously standardized methods, sodium palmitate conjugated with bovine serum albumin (BSA) solution was prepared.[15] Briefly, sodium palmitate dissolved in 1:1 ethanol−water was heated at 70 °C to obtain a 0.5 M concentration solution. Then 2 mM BSA was dissolved in 1 mL of glucose-free DMEM and kept at 40 °C. The prepared sodium palmitate was then added to the BSA solution to give a final FFA/BSA ratio of 6:1, which was close to that of human serum as per the literature. The pH was adjusted to 7.4, and the solution was filtered prior to the experiment.

2.8. Glucose Uptake Assay. The glucose uptake potential of the extract, its fractions, enriched fraction, and isolated compounds was determined using the fluorescent indicator 2-[*N*-(7-nitrobenz-2-oxa-1,3-diazol-4-yl)amino]-2-deoxy-D-glucose (2-NBDG).[16] The cells were treated with various concentrations (1, 10, 25, 50, and 75 μg/mL) of plant extract and its fractions followed by addition of 0.75 mM BSA conjugated palmitate (free fatty acid, FFA) after 2 h. The treated cells were kept in an incubation for 8 h. One hour before terminating the incubation, insulin (100 nM) was added to the cells followed by addition of 2-NBDG after 30 min. The cells were lysed using Triton X-100 and DMSO. The fluorescence expressed by 2-NBDG was measured at excitation/emission wavelengths of 470/530 nm. Glucose uptake was calculated from observed fluorescence data in terms of the fold change of glucose uptake with respect to the control (untreated cells).

2.9. ROS Scavenging Activity. The reactive oxygen species (ROS) inhibition assay was conducted using the fluorescent dye 2′7′-dichloroflourescein-diacetate (H$_2$DCFDA) following the standard protocol.[17] Briefly, the cultured myotube cells, treated with plant extract and fractions followed by FFA or TBHP (after 2 h), were washed with 1× phosphate-buffered saline (PBS) containing 4% FBS. The myotubes were then incubated in the dark in the presence of 5 μM H$_2$DCFDA. After half an hour, the cells were again washed with 1× PBS and lysed with 1% Triton X-100 and DMSO. The homogeneously mixed cell suspension was transferred into a 96-well black plate, and the fluorescence was measured at excitation/emission wavelengths of 480/530 nm.

For flow cytometry analysis of ROS generation, the cell lysates were collected into fluorescence-activated cell sorting (FACS) tubes, and the analysis was carried out in FACSMelody.

2.10. Preparation of the Enriched Fraction. Based on the glucose uptake and ROS scavenging activity, the most active ethyl acetate fraction was further subjected to column chromatography for the isolation of molecules. Twenty grams of ethyl acetate fraction was chromatographed in a silica column (mesh size 100−200) using chloroform and methanol as the eluting solvents. Four subfractions were obtained, hereafter referred to as SF1 (100% chloroform), SF2 (20% methanol in chloroform), SF3 (30% methanol in chloroform), and SF4 (40% chloroform). Based on HPLC and TLC analysis, subfraction 3 (SF3) was further subjected to column chromatography. Silica column (230−400 mesh size) was packed in *n*-hexane, and chloroform was slowly introduced. After sufficient chloroform was eluted, methanol was introduced as an eluting solvent with an increasing gradient of 2% to obtain six subfractions. All the subfractions were examined for their bioactivity, and subfraction C (EFr) showed the best activity, which was then targeted for isolation of active/marker compounds. EFr was further HPLC purified to obtain four compounds.

2.11. HPLC-DAD Analysis of Enriched Fraction and Isolation of Compounds. The active subfraction EFr was HPLC analyzed in a Shimadzu LC-20 AD HPLC system fitted with a Prominence PDA detector. A Discovery RP C-18 analytical (Supelco, 5 μm, 250 × 4.6 mm) column was used for the analytical HPLC experiments of the enriched fraction. Isolation of compounds was carried out in a Supelco C-18 semipreparative column (10 μm, 250 × 10 mm). Trifluoro-acetic acid (TFA, 0.1%) in water (solvent A) and methanol (solvent B) was used as a mobile phase with flow rates 1n and 4 mL/min for analytical and semipreparative HPLC, respectively, over a linear gradient of 25 min.

2.12. Quantitative HPLC Analysis of Enriched Fraction. The active subfraction EFr was enriched with four compounds. Quantitative HPLC analysis was performed to standardize the enriched active fraction with respect to the isolated compounds. Standard stock solutions of 2 mg/mL were prepared for each of the isolated compounds and further diluted to obtain desired test concentrations. Calibration curves were prepared using the HPLC conditions mentioned earlier for qualitative analysis. Concentration vs area curves were plotted in MS Excel 2010 (Figure S2), and the concentration of isolated compounds in the enriched fraction was calculated.

2.13. Identification of Isolated Compounds. The marker compounds isolated from the active enriched fraction

were identified with the help of LCMS/MS and NMR spectroscopy. The full screen mass spectrum of the isolated compounds was recorded in a triple quadruple mass spectrometer with ion source ESI from Thermo Scientific. The sample was prepared in methanol (1 mg/mL) and screened in both positive and negative modes m/z 150−1500 amu with automatic gain control target with a resolution of 70,000.

A Bruker Avance 400 MHz instrument was used for recording of ^{1}H and ^{13}C nuclear magnetic resonance (NMR) spectra. Chemical shifts are presented in δ ppm.

2.14. Immunoblotting Analysis. Cells treated with EFr and compound quercetin-3-glucoside were lysed using the radioimmunoprecipitation assay (RIPA) buffer (50 mM Tris pH 8, 150 mM NaCl, 1% NP-40, 0.5% deoxycholic acid, 0.1% SDS) consisting of phenylmethylsulfonyl fluoride (PMSF) and Halt protease. The cells were centrifuged for 30 min at 14,000 rpm to collect the protein from the lysate, and protein estimation was carried out using a BCA protein estimation kit from Thermo Scientific. The protein mixtures were resolved using 10% sodium dodecyl sulfate−polyacrylamide gel electrophoresis (SDS-PAGE), and separated protein bands were transferred into nitrocellulose membranes (Bio-Rad, Germany). To prevent unspecific binding, the blots were blocked for 40 min using 1% bovine serum albumin (BSA) and incubated with primary antibodies SIRT1 (1:1000), AMPK (1:1000), pAMPK (1:1000), GLUT4 (1:1000), and PGC1-α (1:1000). After overnight incubation, the membranes were washed with TBST solution (50 mmol/L tris-HCl, pH 7.6, 150 mmol/L NaCl, 0.1% Tween 20). Further incubation with the HRP-linked secondary antibody was performed in 1:5000 dilution at room temperature. Ultrasensitive ECL Western blotting detection substrate (BIO-RAD, Germany) was applied to develop the blotted membranes, and the intensity of each band was detected using Adobe Photoshop CS5 (histogram).

2.15. Statistical Analysis. The statistical analysis was performed using one-way ANOVA followed by t test with using the Sigma Plot software. The Student−Newman−Keuls method was used for comparison of the groups. A value of $p < 0.05$ was considered to be significant.

2.16. Target and Ligand Preparation for Molecular Docking and Stimulation Studies. The experimental crystal structure of SIRT1 protein was procured from the RCSB PDB (Research Collaboratory for Structural Bioinformatics Protein Data Bank) portal (https://www.rcsb.org/structure/5BTR). This structure possessed an exogenous ligand resveratrol cocrystallized with the protein. All heteroatoms, including resveratrol and water molecules, were deleted from the PDB protein structure.

The ligand, i.e, quercetin-3-O-glucoside, was obtained from PubChem website (CID_44259136) (https://pubchem.ncbi.nlm.nih.gov/compound/44259136). It was then subjected to geometry optimization in Gaussian09 utilizing DFT (density functional theory) methods and B3LYP functional with the 6-31g (d,p) basis set.[18] The optimum energy conformation of the ligand was then used for docking investigations.

2.17. Molecular Docking. AutoDock 4.2 was employed for docking studies, which predicts the binding energy of small molecules to target proteins.[19] SIRT1 and quercetin-3-O-glucoside were processed using AutoDock tools, wherein all polar hydrogen atoms were added to the structures and Gasteiger charges were computed. AutoDock performs docking calculations employing a grid-based methodology.[20]

The grid box was located at the active site where resveratrol was cocrystallized with specifications of the grid box as- grid box center (−61.146, 87.557, 10.089); grid points in x dimension = 50, grid points in y dimension = 47, grid points in z dimension = 47; and grid point spacing = 0.500 Å. Following AutoGrid calculations and using default docking parameters, the final AutoDock calculations were performed employing the Lamarckian genetic algorithm as the scoring function. The ligand docking pose with the best energy was used further for molecular dynamics simulation.

2.18. Molecular Dynamics Simulation. To measure the stability of SIRT1/ligand complex, molecular dynamics simulation studies were done using the GROMACS 2022 software.[21] The CHARMM (Chemistry at Harvard Macromolecular Mechanics) 36 force field was used to estimate the protein/ligand environment.[22] The topology file for the protein was built using the pdb 2gmx code and that for ligand using the CgenFF (CHARMM general Force Field) server that produces CHARMM compatible topologies for small molecules.[23] The complex was deposited inside a dodecahedral box followed by solvation with TIP3P water[24] and addition of Na$^+$ ions to neutralize the system. To get rid of steric collisions, energy minimization was performed applying the steepest decent method, and the energy of the system was minimized up to −3.23e^{06} (kJ/mol). Then the system proceeded to equilibration processes using the NVT ensemble followed by the NPT ensemble. NVT equilibration was performed for 100 ps to establish the temperature close to 300 K, whereas a 1 ns time was required for NPT equilibration to bring the pressure closest to 1 atm. Finally, the system was subjected to unrestrained production mdrun for 100 ns. The PME (particle mesh Ewald) algorithm was applied for long-range electrostatic interactions.[25] Nonbonded forces were truncated using the Verlet cutoff algorithm at 1.2 nm.[26] Coordinates were extracted at an interval of 10 ps for the 100 ns mdrun.

3. RESULTS AND DISCUSSION

3.1. DPPH Radical Scavenging Activity of *L. leucocephala* Extract and Fractions. The DPPH assay was performed to determine the antioxidant activity of *L. leucocephala* crude extract and fractions using ascorbic acid as positive control. The values of IC$_{50}$ of the crude extract and fractions were compared. Compared to the crude extract (60.0 (SD = 2.9) μg/mL), both the ethyl acetate and *n*-butanol fraction had lower IC$_{50}$ values (33.1 (SD = 2.5) and 34.8 (SD = 3.4) μg/mL), whereas the water fraction presented a greater value (69.4 (SD = 5.0) μg/mL) as evident from Table 1.

3.2. *In Vitro* Glucose Uptake Assay of *L. leucocephala* Extract and Fractions. Based on the cell viability assay on the C2C12 muscle cell line (Figure S1), the maximum nontoxic concentration of the *L. leucocephala* crude extract was

Table 1. IC$_{50}$ Values of *L. leucocephala* Crude (LLME) and Fractions Ethyl Acetate (EAF), *n*-Butanol (BF), and Water (WF); n = 3

sample	IC$_{50}$, mean (SD) (μg/mL)
LLME	60.0 (2.9)
EAF	33.1 (2.5)
BF	34.8 (3.4)
WF	69.4 (5.0)
ascorbic acid	11.3 (1.0)
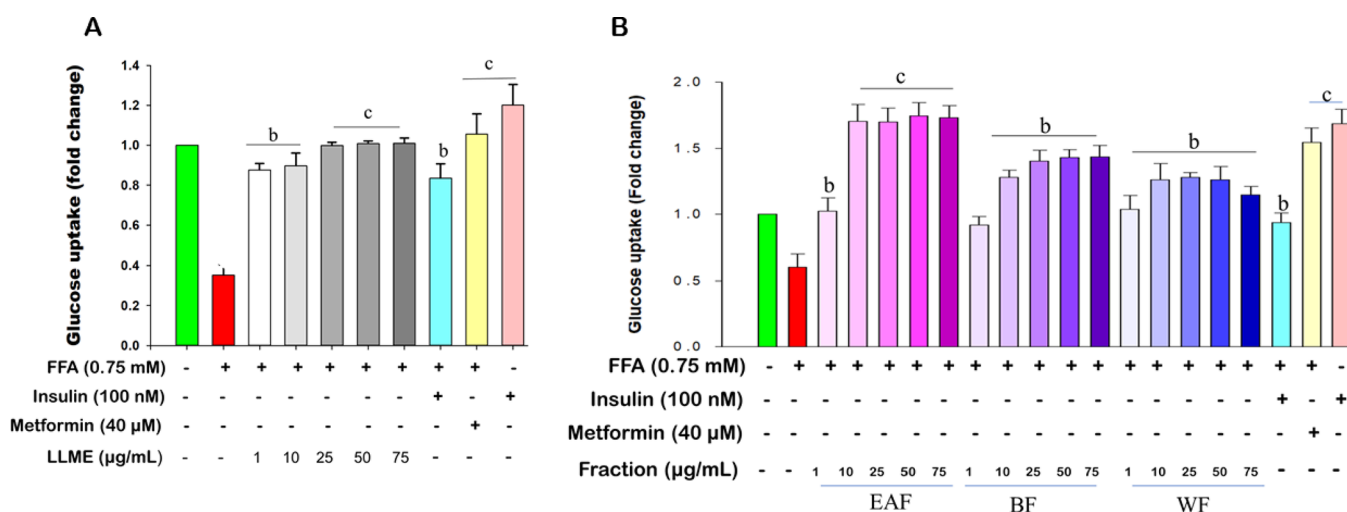
Figure 1. Effect of *L. leucocephala* (A) crude extract (LLME) and (B) fractions ethyl acetate (EAF), *n*-butanol (BF), and water (WF) on the glucose uptake of C2C12 muscle cell line (mean ± SD, *n* = 3). Significant difference from FFA-treated group, a = $p < 0.05$, b = $p < 0.01$, and c = $p < 0.001$.
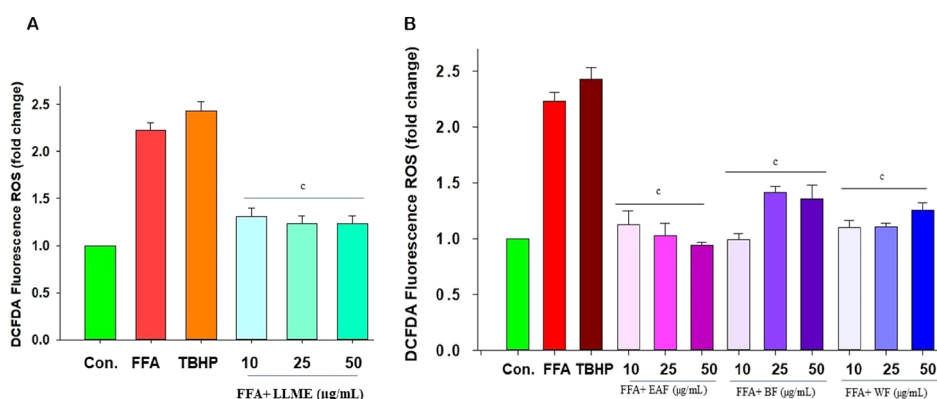

Figure 2. ROS inhibition activity of *L. leucocephala* (A) crude extract (LLME) and (B) fraction EAF, BF, and WF in C2C12 myotubes (mean ± SD, *n* = 3). Significant difference from the FFA-treated group: a = $p < 0.05$, b = $p < 0.01$, and c = $p < 0.001$.

found to be 100 µg/mL (Figure S1A). To assess the efficacy of *L. leucocephala* in skeletal muscle, a glucose uptake assay was performed in free fatty acid (FFA) induced insulin resistance in C2C12 mouse skeletal muscle cell line using 2-NBDG (2-(*N*-(7-nitrobenz-2-oxa-1,3-diazol-4-yl) amino)-2-deoxyglucose). Treatment with FFA downregulated the glucose uptake capacity of the cells compared to FFA untreated control group (0.6-fold), which was observed to be increased by up to 1.4-fold (*$p < 0.05$) upon treatment with crude LL extract in a dose-dependent manner (Figure 1A). The different fractions of the plant extract were also tested against glucose uptake activity, and EAF was found to be the most active as shown in Figure 1B, with 10 to 75 µg/mL concentrations being the most significant in enhancing glucose uptake by the muscle cells up to 1.7-fold (*$p < 0.05$) (with respect to the FFA-treated group).

3.3. ROS Scavenging Activity of *L. leucocepahala* Extract and Fractions. Oxidative stress has been reported to be one of the key factors in the progression of insulin resistance, contributing to both cell damage and anomalies in signaling pathways.[27] The encouraging activity of *L. leucocephala* extract and its fractions in enhancing glucose uptake in the skeletal muscle cell further motivated us to investigate its oxidative stress ameliorating potency. *L.*

leucocephala crude extract and the fractions significantly reduced the ROS generation (Figure 2A,B, respectively) in the treated cells compared to the FFA-treated and TBHP-treated cells (*$p < 0.001$). The EAF showed the most significant ROS scavenging activity (*$p < 0.001$) comparable with the control even at the lowest concentration of 10 µg/mL.

3.4. Preparation and Bioactivity Investigation of *L. leucocephala* Enriched Fraction. The ethyl acetate fraction (EAF) of *L. leucocephala* was found to be the most active in the *in vitro* glucose uptake assay (Figure 1B). ROS scavenging activities also demonstrated encouraging results (Figure 2B). EAF was thus further subjected to column chromatography for the bioactivity guided isolation of active constituents. All the subfractions were screened through *in vitro* glucose uptake activity (data in Figure S3), and subfraction C was found to be most significantly active one for its antihyperglycemic activity. Subfraction C, enriched with four marker compounds, has been denoted as the enriched fraction (EFr), and its activity in C2C12 myotubes was investigated (Figure 5A). The i*n vitro* ROS scavenging assay performed with the prepared enriched fraction (EFr) showed significant activity up to 1.1-fold with respect to FFA-treated cells, which is comparable to the control (Figure 3A). EFr was further investigated for ROS scavenging activity through flow cytometric analysis to obtain
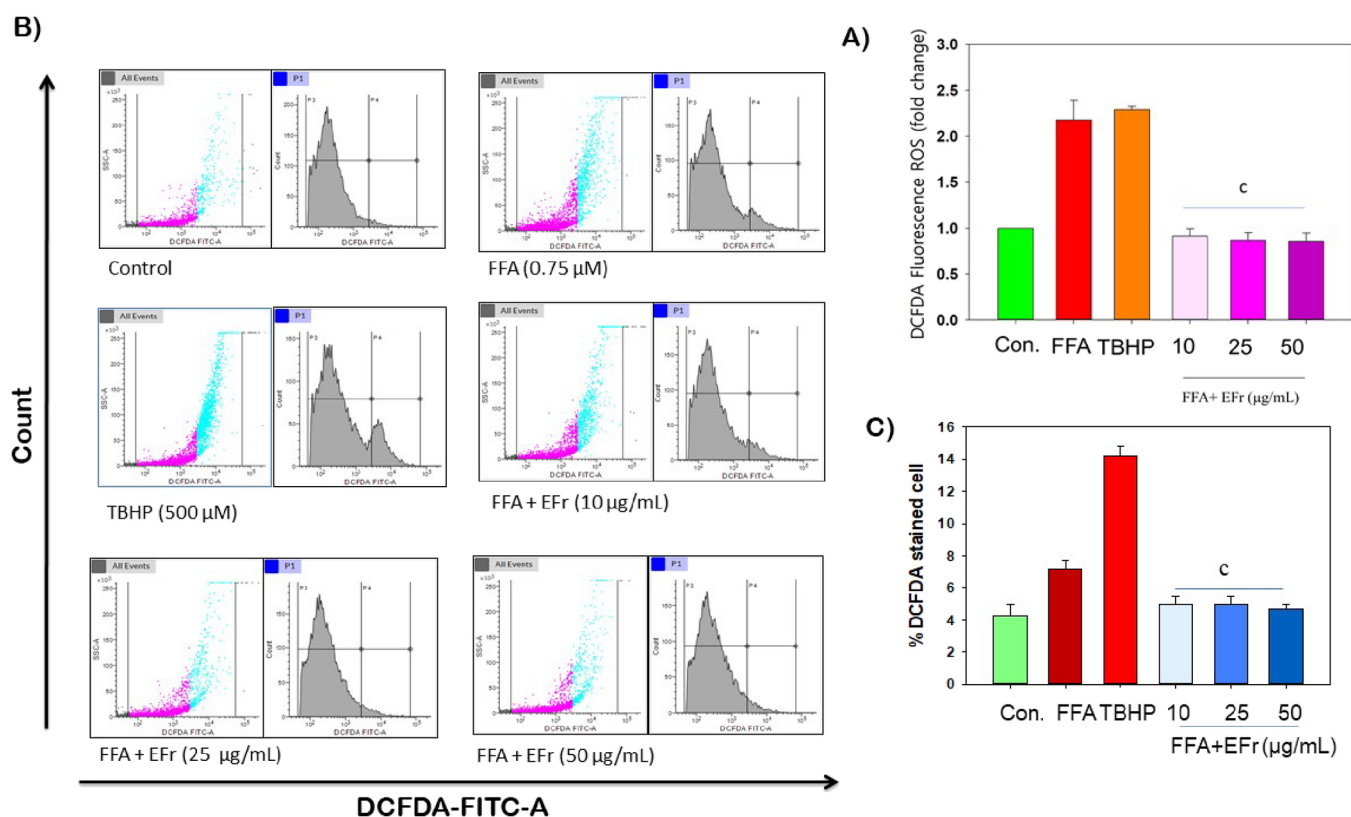
Figure 3. Effect of *L. leucocephala* enriched fraction (EFr) (A) on ROS generated at C2C12 myotubes and (B) H₂DCFDA fluorescence intensity measured in flow cytometry in insulin-resistant C2C12 myotubes. (C) Graphical representation. Data are mean ± SD, $n = 3$. Significant difference from the FFA-treated group: a = $p < 0.05$, b = $p < 0.01$, c = $p < 0.001$.

confirmatory results (Figure 3B,C). Oxidative stress was tested in terms of ROS generated by the DCF fluorescence indicator in insulin-resistant C2C12 myotubes. Treatment with the free fatty acid (FFA, 0.75 mM) causes significant generation of ROS in the myotubes, which is comparable to that generated with TBHP treatment, inferred from the enhanced green fluorescence observed (Figure 3B).

3.5. Isolation and Identification of Active Constituent from Enriched Fraction of *L. leucocephala*. HPLC analysis (Figure 4A) showed that EFr was enriched with two major constituents along with two compounds of intermediate concentration. All four compounds were purified using reversed-phase HPLC and processed for identification (Figure 4B−E).

Isolated compounds were identified by comparing their NMR and mass spectrometric data with those reported in the literature. Analysis of the carbon-13 NMR spectra of all the four compounds indicated the characteristic spectra of flavonoid predicting the nature of the compounds.[28] Further, the compounds were identified through comparison of their spectroscopic data to the reported literature (Tables S1−S4).

Compound **1** (21.183) was found to have a deprotonated $[M − H]^−$ ion at m/z 457.2529 and a prominent peak at m/z 459.2533 in the positive ionization corresponding to the protonated ion of a compound with molecular formula $C_{22}H_{18}O_{11}$. The ESI-MS/MS analysis showed the most intense peak at m/z 169.0800 corresponding to the presence of the gallate moiety. The presence of a signal at m/z 125.0700 and 305.18 00 further confirmed the aromatic core of a catechin gallate.[29] The structure was further validated with the help of the ¹H and ¹³C NMR spectra (data in Table S1), which

corresponds to the reported data of the molecule epigallocatechingallate (EGCG).[29,30]

Compound **2**, isolated as a bright yellow powder (rt 20.780), showed a $[M − H]^−$ deprotonated molecular ion peak at m/z value 463.2652. Further ¹H and ¹³C NMR spectroscopic data for the compound match those reported[31,32] for quercetin-3-*O*-glucoside (Table S2) with molecular formula $C_{21}H_{20}O_{12}$ (exact mass 464 g/mol).[32]

Compound **3**, at rt 17.335, isolated as a pale-yellow solid was identified to be another flavonoid compound from spectroscopic data.[33] The LC−MS/MS data showed an intense peak at 578.3024 in the negative ionization mode. Further comparison of the ¹H and ¹³C NMR data (Table S3) with the reported literature identified the compound to be the rhamnoglucoside naringin.[34] Isolated compound **4** showed a deprotonated molecular ion peak at m/z 301.0030. Comparison of the NMR data for the compound (Table S4) with the reported literature[32] identified the compound to be flavonoid quercetin.[35]

3.6. HPLC Quantification of the Enriched Fraction EFr. The HPLC spectra of the bioactively enriched fraction showed four prominent peaks (Figure 4A), which were quantified using HPLC fitted with a PDA detector. The most abundant compounds **1** and **2** were found to be present at concentrations of 431.91 and 397.96 mg/g in EFr, whereas compound **3** and **4** were present at concentrations of 154.73 and 145.82 mg/g, respectively. The concentrations of the isolated compounds in the enriched fraction are presented in Table 2.

3.7. Effect of Enriched Fraction of *L. leucocephala* on SIRT1/AMPK/GLUT4/PGC1-α Protein Expression. The
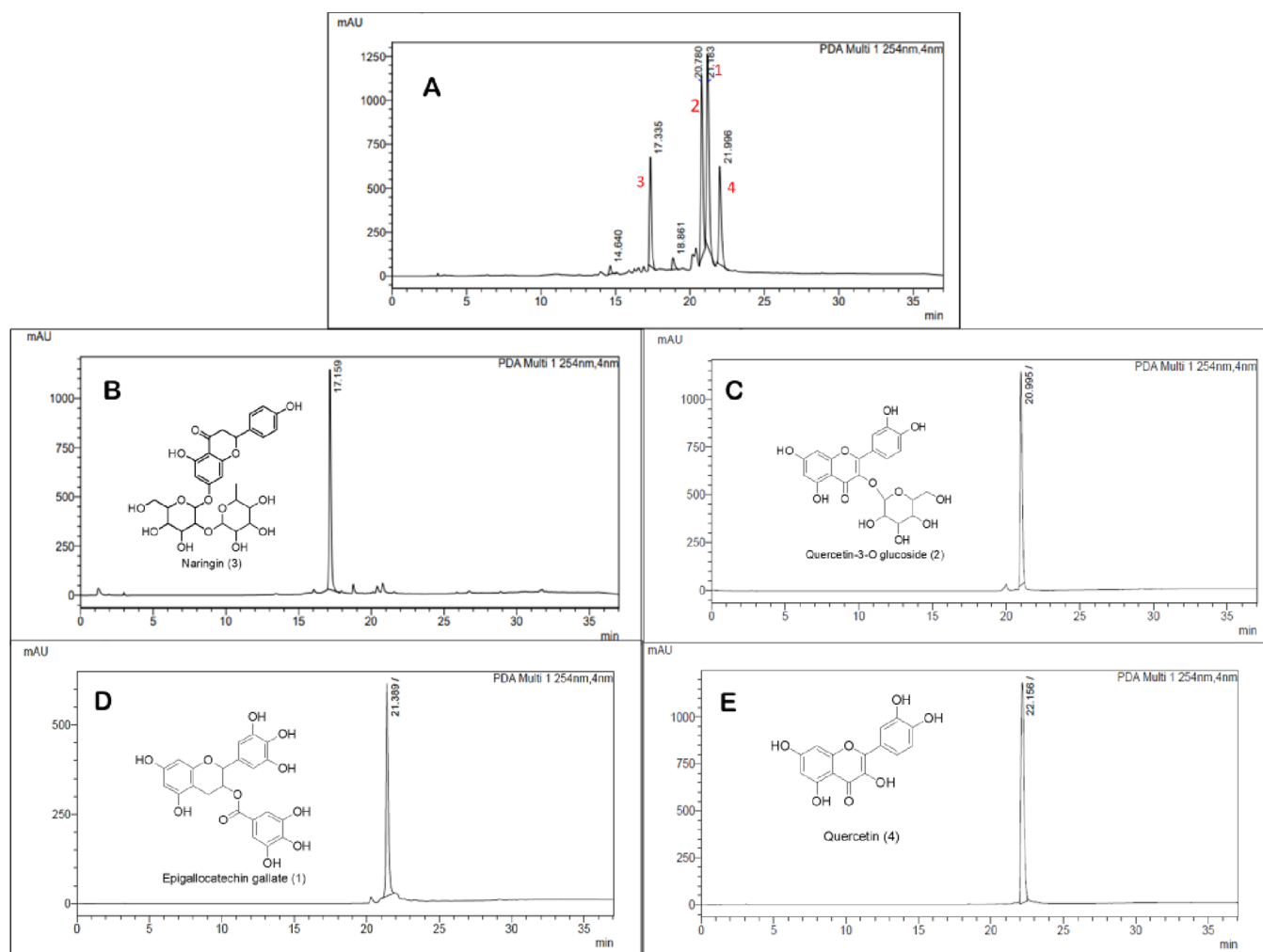
Figure 4. HPLC chromatogram of (A) enriched fraction EFr of *L. leucocephala* and its isolated compounds (B−E).

Table 2. Concentrations of Isolated Pure Compounds in the Bioactive Enriched Fraction EFr

compound	concentration (mg/g) in EFr	purity of compound (%)
epigallocatechin gallate (1)	431.91	99.13
quercetin-3-glucoside (2)	397.96	98.23
naringin (3)	154.73	98.98
quercetin (4)	145.82	99.50

study investigated the effect of EFr on the GLUT4 translocation pathway associated with insulin resistance in skeletal muscle using C2C12 myotubes. FFA treatment downregulated the expressions of SIRT1 and GLUT4 and decreased the phosphorylation of AMPK (Figure 5). EFr treatment upregulated the SIRT1 protein expression at a concentration of 50 μg/mL of dose (Figure 5B) and stimulated GLUT4 translocation in palmitate-treated myotubes (Figure 5E).

3.8. Bioactivity Assessment of Isolated Molecules. The glucose uptake potential and ROS scavenging activity of the four isolated molecules were screened in FFA-induced C2C12 myotubes. The cells were treated with 1−25 μg/mL concentration of each of the compounds, which were converted to μM concentration for each of the individual molecule. All the four compounds showed positive glucose uptake activity (Figure 6A) with compounds EGCG (1) and quercetin-3-glucoside (QG, 2) showing the most significant results (*$p < 0.001$). QG showed positive glucose uptake from concentration 2.1 μM, whereas EGCG showed significant results from 10.9 μM concentration. Further, a comparative study of the FFA-induced ROS scavenging activity of the compounds demonstrated (Figure 6B) that QG has the most significant ROS inhibition activity (*$p < 0.001$) in a dose-dependent manner followed by EGCG with values *$p < 0.002$ for lower concentrations and *$p < 0.001$ for higher concentrations. Thus, QG was further taken up for mechanistic study using immunoblotting and molecular dynamics simulations.

3.9. Effect of Quercetin-3-glucoside on the SIRT1/ AMPK/GLUT4 Pathway. The positive glucose uptake and ROS scavenging results of quercetin-3-glucoside further drew forth the immunoblotting investigation to observe the effect of the compound on the SIRT1 protein. The same was observed in the FFA-treated C2C12 muscle cell line. Palmitate treatment reduced SIRT1 expression, which was significantly upregulated up to 1.2−1.6-fold by different concentrations of QG. Further, QG showed a significant effect on the phosphorylation of AMPK (1.2−1.4-fold) and stimulated GLUT4 translocation (1.9−2.4-fold) in the myotubes (Figure 7).
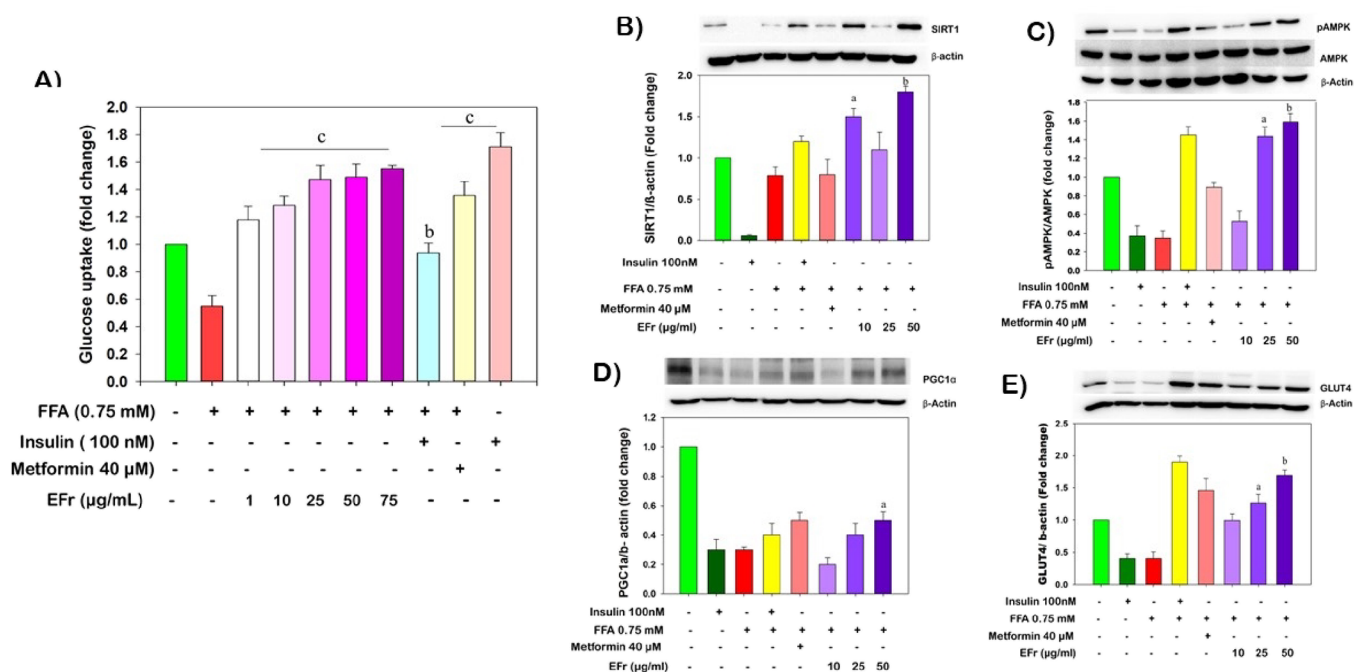
Figure 5. Effect of *L. leucocephala* enriched fraction (EFr) (A) on the glucose uptake of insulin-resistant C2C12 muscle cells and on the expression of the SIRT1/AMPK/GLUT4 pathway of glucose metabolism (B−E). Data as mean ± SD, $n = 3$. Significant difference from FFA-treated group: a = $p < 0.05$, b = $p < 0.01$, and c = $p < 0.001$.
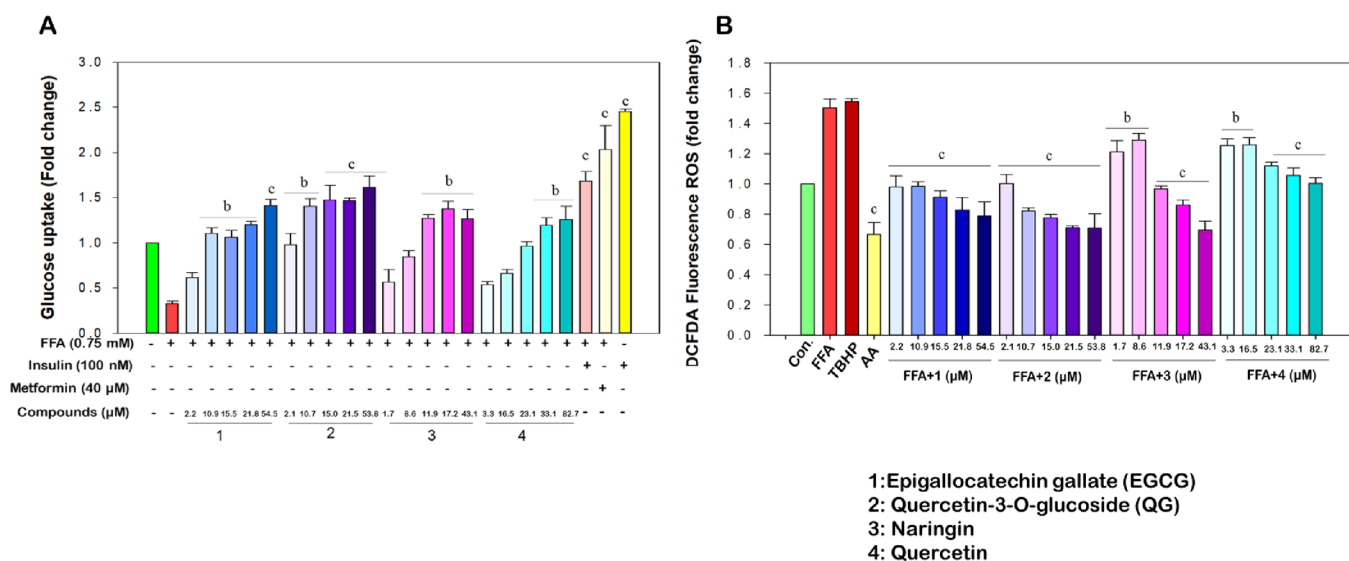

Figure 6. Effect of *L. leucocephala* isolated compounds in (A) glucose uptake activity and (B) the FFA-induced ROS inhibition activity in C2C12 myotubes (mean ± SD, $n = 3$). Significant difference from FFA-treated group: a = $p < 0.05$, b = $p < 0.01$, c = $p < 0.001$.

3.10. Molecular Docking Study of QG (Quercetin-3-glucoside) with SIRT1 Protein. Molecular docking study was performed to explore the binding affinity of QG with the SIRT1 protein structure. The optimized structure of quercetin-3-glucoside procured from Gaussian09 is presented in Figure 8A. Optimization of molecules before beginning any study is necessary as it provides optimum energy structures that are stable and resemble original structures found in the environment. The ligand binding zone of SIRT1 is depicted in Figure 8B.

QG was associated with a negative binding energy of −6.3 kcal/mol in the active zone of SIRT1. The best docked pose of the ligand in the binding zone of the receptor is shown in

Figure 9A. The ligand interacted considerably with the active site residues of SIRT1 through hydrogen bonds and hydrophobic pi-alkyl contacts, as depicted Figure 9B. The dihydroxyphenyl ring of quercetin formed two hydrogen bonds with the carboxyl side chain of Glu230. A pi-donor hydrogen bond was seen between the phenyl ring and Asn226. Additionally, another H-Bond was constituted by an OH of the benzene ring of quercetin with Gln222. Reinforcing these bonds, pi-alkyl bonds of longer range were observed with residues like Ile223, Arg446, and Pro447.

3.11. Molecular Dynamics Simulation. To estimate the stability of the solvated SIRT1/quercetin-3-glucoside complex, MD simulations were implemented for 100 ns. Root mean
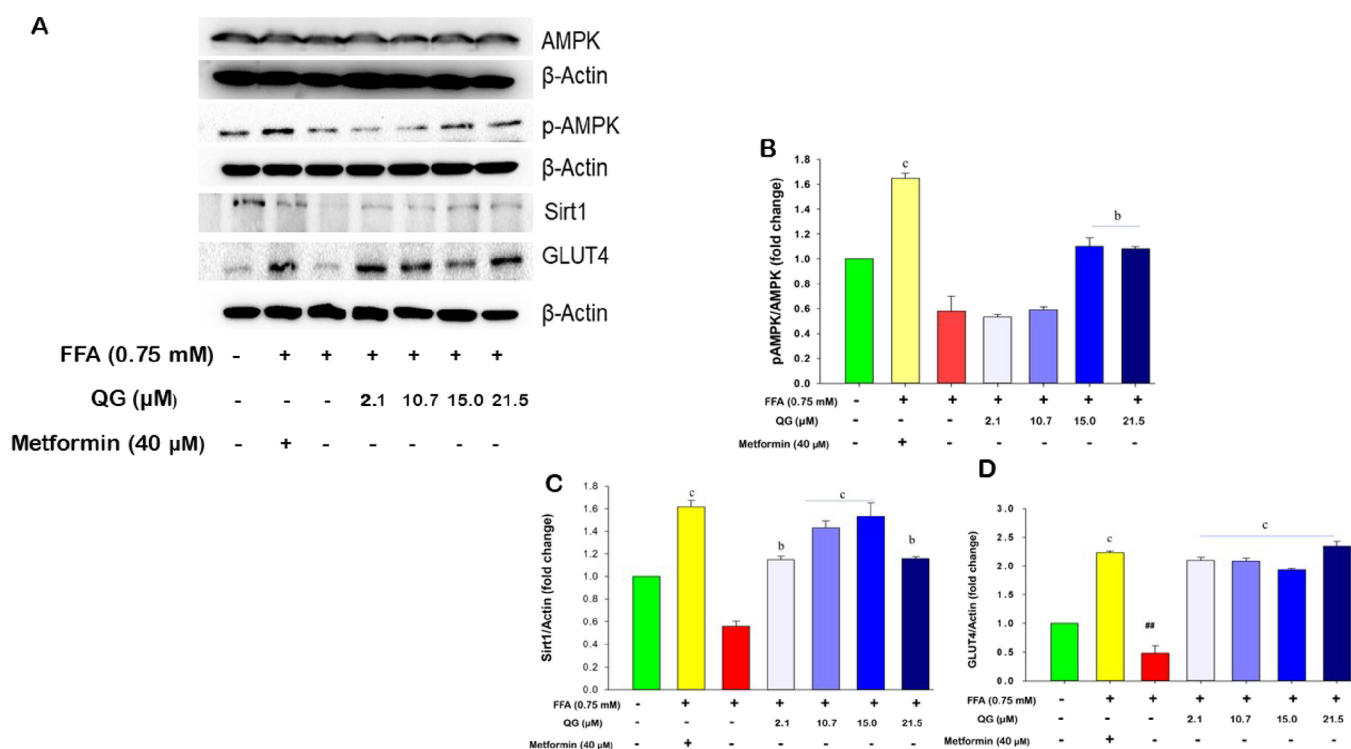
Figure 7. Effect of QG on the protein expression of proteins associated with the SIRT1/AMPK/GLUT4 pathway of glucose metabolism (A–D). Data as mean ± SD, $n = 3$. Significant difference from FFA-treated group, a = $p < 0.05$, b = $p < 0.01$, and c = $p < 0.001$.
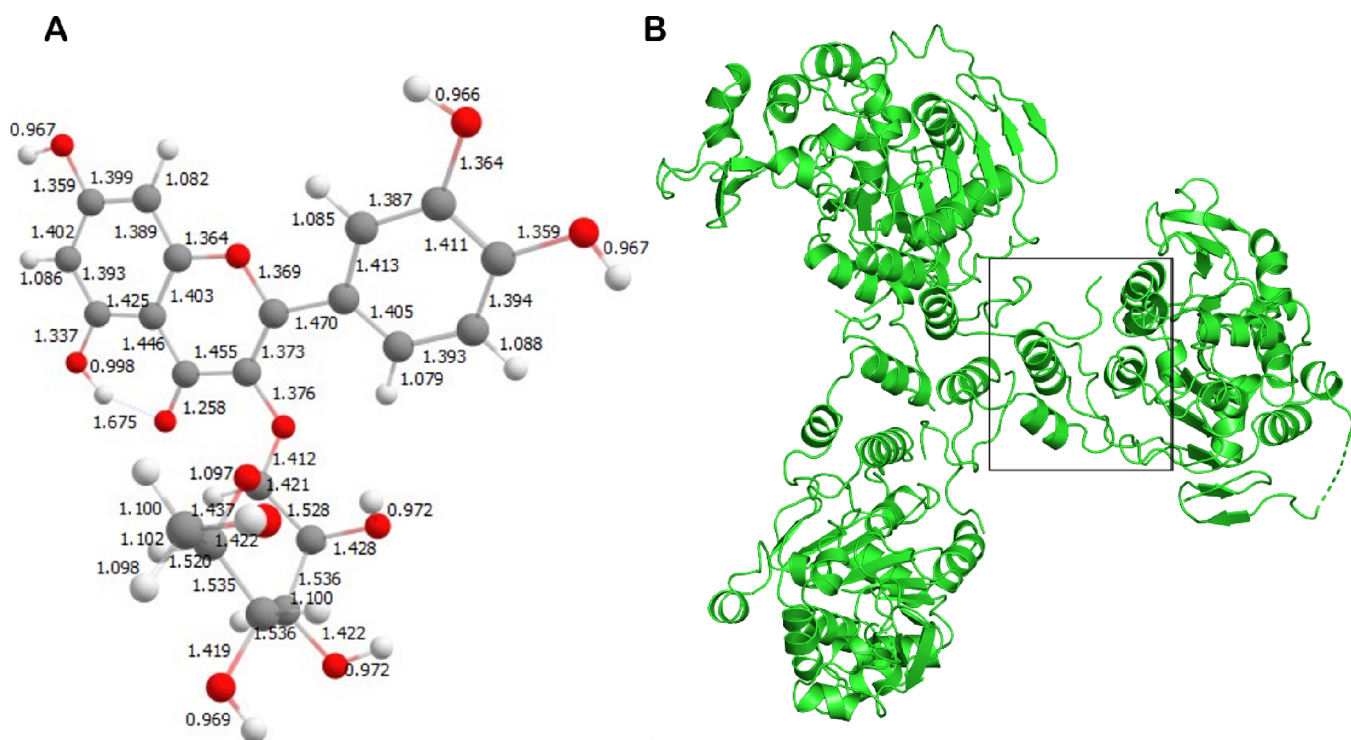

Figure 8. Optimized geometry of (A) quercetin-3-O-glucoside. The number denotes bond lengths (Å). (B) SIRT1 protein. The black box denotes the active inhibitor binding zone of SIRT1 protein.

square deviation (RMSD) studies of the SIRT1 backbone and the ligand dictated the stability profiles of the MD simulation. Chain B of the trimeric SIRT1 backbone was equilibrated from about 44 ns, exhibiting values close to 0.65 nm (Figure 10A). The ligand exhibited RMSD near 0.20 nm toward the last 25 ns of the simulation (Figure 10B).

Radius of gyration (Rg) studies measure how compact a protein conformation remains during the simulation. SIRT1 when complexed with the quercetin glucoside persisted in a compact form for the 100 ns simulation as observed from the Rg plot in Figure 11A. The root mean square fluctuation (RMSF) plot shows fluctuation of residues from their
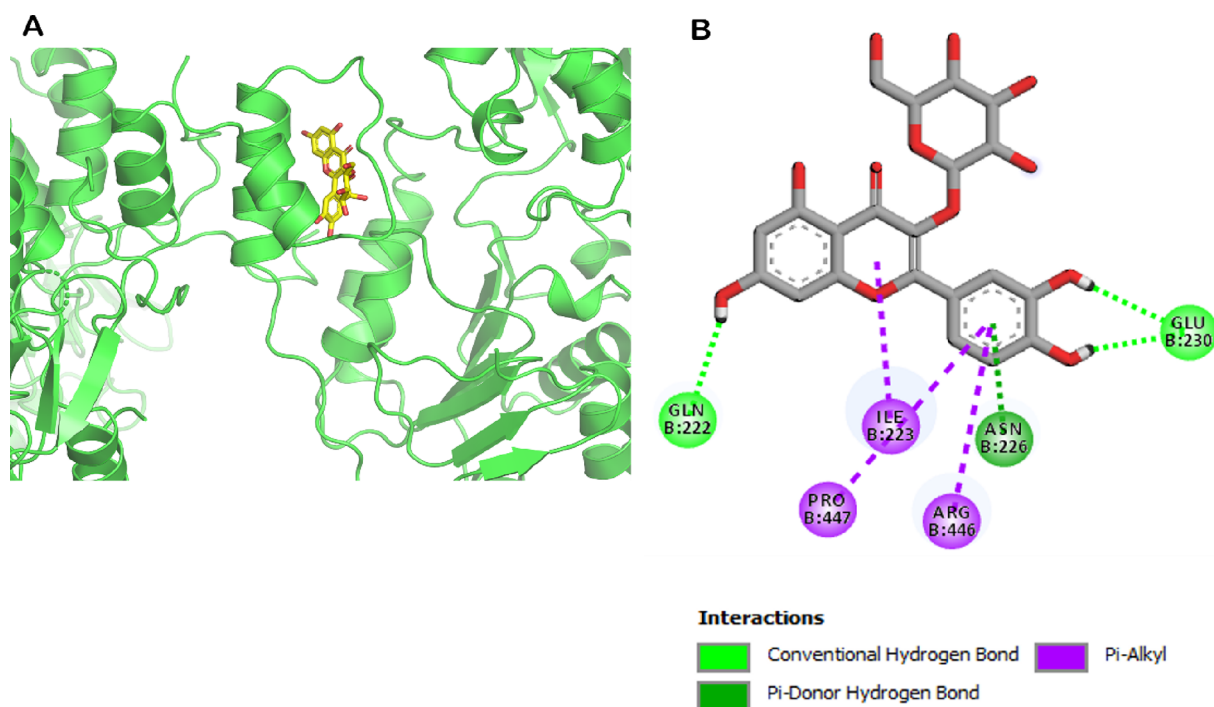
Figure 9. (A) The best docked conformer of quercetin-3-*O*-glucoside. (B) Interactions of the ligand with the binding site residues of SIRT1.
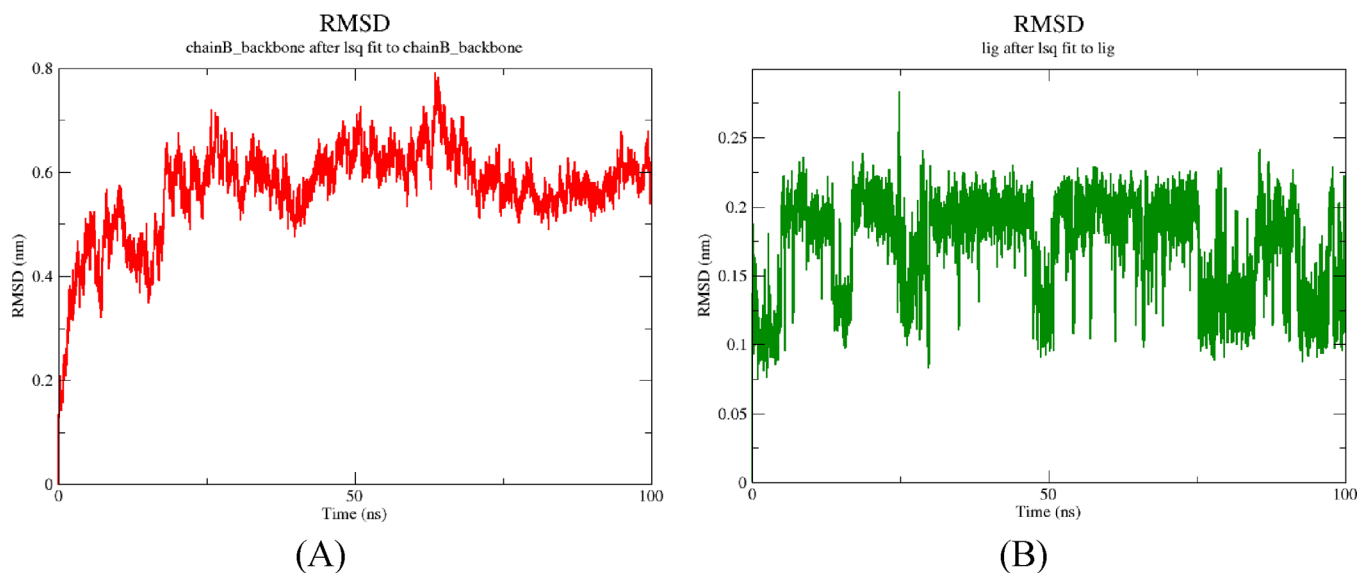

Figure 10. RMSD graph of the (A) SIRT1 backbone and (B) quercetin-3-*O*-glucoside of 100 ns simulation trajectory.

respective means over 100 ns. From the RMSF plot, it can be noticed that there is diminished fluctuation near residues Glu230, Asn226, and Ile227, which might be due to the association of these residues with the ligand (Figure 11B).

Hydrogen bonds were formed between the ligand and SIRT1 active site dominantly with amino acids like Glu230, Asn226, and Ile227. Both the OH functional groups of the phenyl ring in quercetin-3-*O*-glucoside consistently formed H-bonds with the Glu230 carboxyl side chain that were present for around 47.41 and 48.28% of the time of 100 ns. Similarly, Asn226 and Ile227 also formed two noticeable interactions, respectively, with the pyrone ring O atom and phenyl OH of the ligand with 24.74 and 24.30% occupancy. These interactions are displayed in Figure 12.

Polyphenols are a class of secondary metabolites proven to be one of the prominent types of bioactive natural product. The role of polyphenols in the management of insulin resistance has been widely studied. A subcategory of the broad range of polyphenolic compounds is the flavonoids, characterized by the presence of its C6−C3−C6 backbone. Flavonoids have been found to possess many beneficial bioactivities in managing oxidative stress, inflammation, metabolic health, and cancer.[36] Polyphenols and flavonoids exert their antidiabetic action by protecting pancreatic β-cells and promoting β-cell proliferation along with attenuating oxidative stress and regulating insulin-dependent and -independent signaling pathways. They are also reported to be beneficial in managing other related metabolic symptoms like
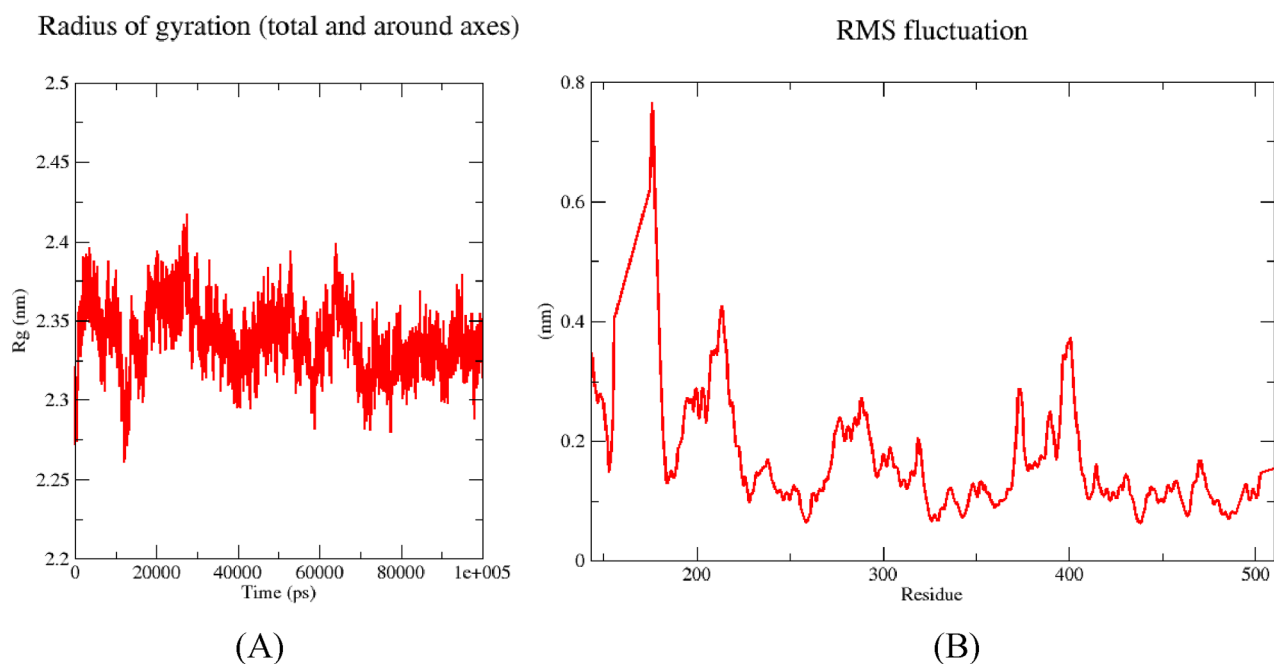
Figure 11. (A) Rg graph of the SIRT1 protein. (B) RMSF plot of SIRT1 residues' backbone atoms.
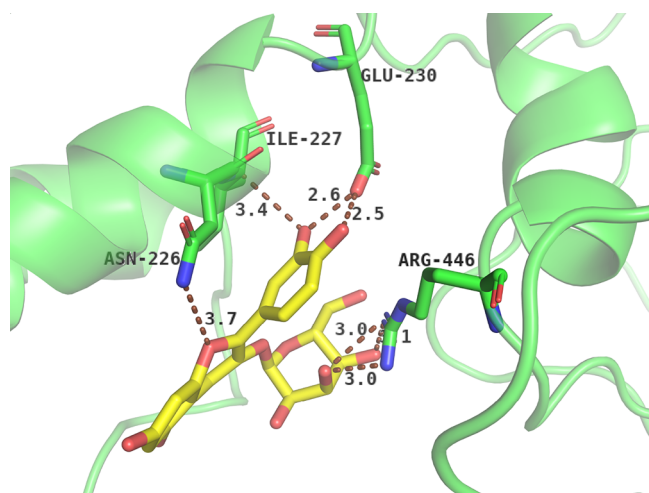
Figure 12. H-bonds formed by the ligand with the active residues of SIRT1.

vascular complications, nephropathy, neuropathy, and retinopathy.[37]

L. leucocephala seeds, leaves, and the aerial parts are found to be rich in bioactive compounds like , phenolics, tannins, and flavonoid glycosides.[8,38] The plant holds a rich place in various ethnic and traditional medicinal systems all over the globe. Still, there are not much reports of phytochemicals being isolated from the plant and their therapeutic effect against various diseases.[39,40] Tyrosinase inhibitory proanthocyanidines have been identified from the leaf and seeds of *L. leucocephala*.[41] The antihyperglycemic properties of different extracts of the plant have also been studied and reported. The aqueous fruit extract upregulated adipogenesis, inhibited lipolysis, and also upregulated glucose uptake in rat adipocytes.[42] The antioxidant activity of the plant has also been explored as a therapeutic option toward lipid peroxidation inhibition, anticancer and cytotoxic activity, and so on.[39,43,44] A glucose binding lectin with hemagglutination

activity against human lymphocyte has also been isolated from the seeds.[45]

The available literature shows that the ethnomedicinal plant *L. leucocephala* has significant potential toward novel therapeutic applications. However, there have been no indepth investigations concerning the phytochemicals responsible for its bioactivity. Although mass spectrometric techniques identify the number of phytochemicals in the plant,[44,46] there is a need to carry out comprehensive bioactivity guided investigation to identify the phytochemicals responsible for its antidiabetic activities and related traditional claims. Besides, marker-assisted standardization of a bioactive-enriched fraction can open up new possibilities toward the development of novel therapeutic applications from the plant. The present study resulted in the identification of four bioactive compounds and the preparation of an enriched fraction with potent antihyperglycemic and ROS scavenging activity from the mature unripe fruits of the plant. The isolated compounds also showed varying degrees of glucose uptake and ROS inhibitory potential when tested *in vitro*.

An *in vitro* glucose uptake study supported the traditional use and claim as an antihyperglycemic agent. Treatment with *L. leucocephala* crude extract and different fractions reversed the insulin resistance caused by FFA treatment and upregulated glucose uptake in C2C12 myotubes. The ethyl acetate fraction showed the most significant bioactivity with an active concentration of 10 to 75 μg/mL (Figure 1B). The most active ethyl acetate fraction also showed *in vitro* radical scavenging activity, IC_{50} 33.10 $\pm$ 2.46 μg/mL (Table 1), and ROS scavenging activity when tested on FFA-induced ROS generation on C2C12 muscle cells (Figure 2B). Following the results of *in vitro* glucose uptake and ROS inhibitory activity, the most active ethyl acetate fraction was further processed, and an enriched fraction was prepared with four marker compounds (Figure 4). Various scientific studies[47] have shown ethyl acetate to be a preferable solvent for the extraction of phenolics and flavonoid compounds,[47,48] which is also supported by the isolated compounds being identified as

different polyphenol and flavonoid compounds. Further, the most active potential of the ethyl acetate fraction is demonstrated by a lower IC50 value, inferring a higher antioxidant activity than the crude extract and other fractions along with more activity in glucose uptake and ROS scavenging assay as elucidated. Four marker compounds were isolated, and the most abundant compound 1, EGCG, a catechin, is one of the major compounds available in green tea. The beneficial properties of EGCG have been well studied and reported in various literature.[49] ECGC have also been reported to show impressive antidiabetic potential in various studies.[50] Two flavonoids were isolated, quercetin-3-glucoside and quercetin, of which quercetin was present in a minor amount in the prepared enriched fraction. Compound 3 isolated is identified to be a flavanone naringin. Flavonoids are well-known for their antidiabetic and other therapeutic properties.[51] The beneficial potential of quercetin-3-O-gluco-side in the management of insulin resistance was also demonstrated in the significant results obtained in the *in vitro* studies conducted. The compound showed significant glucose uptake activity up to 1.2-fold in FFA-induced insulin-resistant C2C12 myotubes over a concentration range of 2−54 μM (1−25 μg/mL). The compound also showed a 0.82-fold (0.66-fold for positive control) ROS scavenging activity even at a concentration of 2.1 μM (1 μg/mL). Quercetin glycosides have been reported to show various therapeutic advantages like nephroprotective, cardioprotective, antioxidant, antidiabetic, and other properties.[52] QG is one of such promising glycosides commonly available in many plants, including dietary consumables. The antidiabetic potential of the compound on STZ-induced diabetic Wister rats has been reported by Jaychandran et al.[53] The same has also been studied as a dipeptidyl peptidase-4 inhibitor in the glucagon-like peptide (GLP)-1 signaling pathway by Zhang et al.[54] Oral admin-istration is the most preferred route for the intake of dietary bioactive compounds. However, the absorption and bioavail-ability of flavonoids vary depending upon their subcategory, glycosylation, esterification, molecular weight, and composi-tion. Flavanones, catechins, and quercetin glucosides are better absorbed than some other classes of flavonoids.[55] It has also been reported that quercetin glycosides have more bioavail-ability than the quercetin aglycone itself.[56] Quercetin glyco-sides, after consumption, are hydrolyzed in the epithelial cell or in the colon to produce quercetin aglycon. This aglycon is then absorbed in the large intestine.[57] In the present study, quercetin-3-O-glucoside showed the most pronounced glucose uptake and ROS inhibitory activity. Further, the compound showed stable interactions with the SIRT1 residue through the formation of hydrogen bonds during molecular docking and stimulation studies. QG further stimulates SIRT1 upregulation and AMPK phosphorylation and upregulates GLUT4 trans-location. Also, the standardized fraction, enriched with 397.96 mg/g of QG along with 431.91 mg/g of EGCG, 154.73 mg/g naringin, and 145.82 mg/g of quercetin, showed regulation of insulin resistance and hyperglycemia following the SIRT1/ AMPK signaling cascade.

The activation of sirtuin, a nicotinamide adenine dinucleo-tide (NAD+)-dependent histone deacetylase, is being identi-fied as a novel therapeutic target for many important biological functions including insulin resistance, type II diabetes, and cardiovascular diseases. SIRT1 is an important factor in a wide range of cellular processes. It plays an important role in the maintenance of inflammation and reduction of oxidative stress,

in turn inhibiting the progression of insulin resistance in insulin-sensitive tissues along with protecting the pancreatic β-cells.[58] It has been demonstrated that deactivation of SIRT1 inhibited insulin-dependent glucose uptake and GLUT4 translocation in 3T3-L1 adipocytes.[57] However, addition of a small molecule SIRT1 activator resulted in the increased glucose uptake and insulin signaling. Gene expressions also showed the inverse relationship of SIRT1 expressions to inflammatory genetic markers.[59] Many natural phytochemicals including polyphenols and flavones are known SIRT1 activators.[60] There are also reports of resveratrol and other polyphenols acting as an antiaging molecule by modulating SIRT1 expression.[61] The EFr enriched with dietary bioactive molecules significantly enhanced the expression of SIRT1, P-AMPKα, and GLUT4 molecules ($p < 0.05$) of the insulin signaling pathway (Figure 5B−E).

This study demonstrated that supplementation of quercetin-3-glucoside and its enriched fraction EFr can improve glucose metabolism through upregulation of the SIRT1/AMPK/ GLUT4 signaling pathway and can improve glucose uptake in insulin-resistant muscle cells. Further, isolated quercetin-3-glucoside showed promising results in insulin sensitivity and GLUT4 translocation when tested *in vitro*. Although the present study explores the role of traditional medicinal plant *L. leucocephala* on glucose uptake and the bioactive molecules involved in the process, further studies involving an animal model and clinical trials can open up new possibilities in supporting the findings of the study. The findings of this study can thus be extrapolated to generate conclusive data regarding the selection of dose for potential therapeutic interventions.

4. CONCLUSIONS

The present study demonstrated the therapeutic potential of the traditionally used plant *L. leucocephala* seed extract and its various fractions on enhancing glucose uptake on the FFA-treated C2C12 muscle cell line, which was in accordance with the ethnobotanical claim of the plant being used for diabetes and related diseases. An enriched fraction prepared from the ethyl acetate fraction further confirmed its usefulness as a potential therapeutic option for the regulation of insulin resistance and diabetes via the modulation of SIRT1/AMPK/ GLUT4 signaling pathways. The enriched fraction was rich in four bioactive polyphenol compounds that were isolated and identified and whose bioactivity was assessed. Further, the enriched fraction has been standardized with respect to the isolated marker compounds, which opens up the possibility of its development toward botanical or phytopharmaceutical drugs. Although this study comprehensively evaluates the bioactivity guided identification of the phytochemicals responsible for the antihyperglycemic activity of *L. leucocephala* plant, further studies are required for the development of novel therapeutic interventions from this important traditional medicinal plant.

■ ASSOCIATED CONTENT

ⓢ Supporting Information

The Supporting Information is available free of charge at https://pubs.acs.org/doi/10.1021/acsomega.3c09672.

Additional experimental details, NMR data of all compounds, and raw data of Western blot (PDF)

AUTHOR INFORMATION

Corresponding Author

Jagat C Borah − *Chemical Biology Laboratory 1, Institute of Advanced Study in Science and Technology (IASST), Guwahati, Assam 781035, India;* ⊙ orcid.org/0000-0001-6876-2659; Phone: +91-361-2273061; Email: borahjc@gmail.com; Fax: +91-361-2273063

Authors

Pranamika Sarma − *Chemical Biology Laboratory 1, Institute of Advanced Study in Science and Technology (IASST), Guwahati, Assam 781035, India; Department of Chemistry, Gauhati University, Guwahati, Assam 781014, India*

Bhaswati Kashyap − *Chemical Biology Laboratory 1, Institute of Advanced Study in Science and Technology (IASST), Guwahati, Assam 781035, India;* Present Address: Vascular Ion Channel Laboratory, Department of Kinesiology and Applied Physiology, University of Delaware, Newark, DE 19713, USA

Shalini Gurumayum − *Chemical Biology Laboratory 1, Institute of Advanced Study in Science and Technology (IASST), Guwahati, Assam 781035, India*

Srutishree Sarma − *Catalysis and Molecular Modelling Laboratory, Department of Chemical Sciences, Tezpur University, Tezpur, Assam 784028, India*

Paran Baruah − *Chemical Biology Laboratory 1, Institute of Advanced Study in Science and Technology (IASST), Guwahati, Assam 781035, India*

Deepsikha Swargiary − *Chemical Biology Laboratory 1, Institute of Advanced Study in Science and Technology (IASST), Guwahati, Assam 781035, India*

Abhipsa Saikia − *Chemical Biology Laboratory 1, Institute of Advanced Study in Science and Technology (IASST), Guwahati, Assam 781035, India*

Ramesh Ch. Deka − *Catalysis and Molecular Modelling Laboratory, Department of Chemical Sciences, Tezpur University, Tezpur, Assam 784028, India;* ⊙ orcid.org/0000-0003-4352-2661

Complete contact information is available at:
https://pubs.acs.org/10.1021/acsomega.3c09672

Author Contributions

Pranamika Sarma: data curation, formal analysis, investigation, methodology, writing − original draft; Bhaswati Kashyap: data curation, formal analysis; Shalini Gurumayum: methodology, investigation, data curation; Srutishree Sarma: methodology, investigation, writing; Deepsikha Swargiary: investigation; Paran Baruah: investigation; Abhipsha Saikia: validation; Ramesh C Deka: review and editing; Jagat C Borah: conceptualization, supervision, project administration, review and editing, resources.

Notes

The authors declare no competing financial interest.

REFERENCES

(1) Tangvarasittichai, S. Oxidative stress, insulin resistance, dyslipidemia and type 2 diabetes mellitus. *World J. Diabetes* **2015**, *6* (3), 456.

(2) Ayer, A.; Fazakerley, D. J.; James, D. E.; Stocker, R. The role of mitochondrial reactive oxygen species in insulin resistance. *Free Radic. Biol. Med.* **2022**, *179*, 339−362.

(3) Herzig, S.; Shaw, R. J. AMPK: guardian of metabolism and mitochondrial homeostasis. *Nat. Rev. Mol. Cell Biol.* **2018**, *19* (2), 121−135.

(4) Sies, H.; Jones, D. P. Reactive oxygen species (ROS) as pleiotropic physiological signalling agents. *Nat. Rev. Mol. Cell Biol.* **2020**, *21* (7), 363−383.

(5) Wang, Y.-M.; Huang, T.-L.; Meng, C.; Zhang, J.; Fang, N.-Y. SIRT1 deacetylates mitochondrial trifunctional enzyme α subunit to inhibit ubiquitylation and decrease insulin resistance. *Cell Death Dis.* **2020**, *11* (10), 821.

(6) Zhu, Y.; Yang, H.; Deng, J.; Fan, D. Ginsenoside Rg5 improves insulin resistance and mitochondrial biogenesis of liver via regulation of the Sirt1/PGC-1α signaling pathway in db/db mice. *J. Agric. Food Chem.* **2021**, *69* (30), 8428−8439.

(7) Heuzé, V.; Tran, G.Leucaena (*Leucaena leucocephala*). Feedipedia, a programme by INRAE, CIRAD, AFZ and FAO, 2015; https://feedipedia.org/node/282.

(8) Zayed, M. Z.; Samling, B. Phytochemical constituents of the leaves of *Leucaena leucocephala* from Malaysia. *Int. J. Pharm. Pharm. Sci.* **2016**, *8* (12), 174−179.

(9) Andrade-Cetto, A.; Heinrich, M. Mexican plants with hypoglycaemic effect used in the treatment of diabetes. *J. Ethnopharmacol* **2005**, *99* (3), 325−348.

(10) Hartanti, D.; Budipramana, K. Traditional antidiabetic plants from Indonesia. *Ethnobot. Res. Appl.* **2020**, *19*, 1−24.

(11) Septina, E.; Yetti, R. D.; Rivai, H. Overview of Traditional Use, Phytochemical, and Pharmacological Activities of Chinese Petai (*Leucaena leucocephala*). *Int. J. Pharm. Sci. Med.* **2020**, *5* (12), 1−10.

(12) Ivorra, M.; Paya, M.; Villar, A. A review of natural products and plants as potential antidiabetic drugs. *J. Ethnopharmacol* **1989**, *27* (3), 243−275.

(13) Sheikh, Y.; Maibam, B. C.; Biswas, D.; Laisharm, S.; Deb, L.; Talukdar, N. C.; Borah, J. C. Anti-diabetic potential of selected ethnomedicinal plants of north east India. *J. Ethnopharmacol* **2015**, *171*, 37−41.

(14) Dzoyem, J. P.; Eloff, J. N. Anti-inflammatory, anticholinesterase and antioxidant activity of leaf extracts of twelve plants used traditionally to alleviate pain and inflammation in South Africa. *J. Ethnopharmacol* **2015**, *160*, 194−201.

(15) Sarma, P.; Bharadwaj, S.; Swargiary, D.; Ahmed, S. A.; Sheikh, Y.; Barge, S. R.; Manna, P.; Talukdar, N. C.; Bora, J.; Borah, J. C. Iridoid glycoside isolated from *Wendlandia glabrata* and the role of its enriched fraction in regulating AMPK/PEPCK/G6Pase signaling pathway of hepatic gluconeogenesis. *New J. Chem.* **2022**, *46* (27), 13167−13177.

(16) Kim, M. S.; Hur, H. J.; Kwon, D. Y.; Hwang, J.-T. Tangeretin stimulates glucose uptake via regulation of AMPK signaling pathways in C2C12 myotubes and improves glucose tolerance in high-fat diet-induced obese mice. *Mol. Cell. Endocrinol.* **2012**, *358* (1), 127−134.

(17) Manna, P.; Jain, S. K. L-cysteine and hydrogen sulfide increase PIP3 and AMPK/PPARγ expression and decrease ROS and vascular inflammation markers in high glucose treated human U937 monocytes. *J. Cell Biochem.* **2013**, *114* (10), 2334−2345.

(18) Frisch, M. J.; Trucks, G.; Schlegel, H. B.; Scuseria, G. E.; Robb; Cheeseman, J. R.; Scalmani, G.; Barone, V.; Mennucci, B.; Petersson, G. A. *Gaussian 09W*, revision A. 02. 2009.

(19) Morris, G. M.; Huey, R.; Lindstrom, W.; Sanner, M. F.; Belew, R. K.; Goodsell, D. S.; Olson, A. J. AutoDock4 and AutoDockTools4: Automated docking with selective receptor flexibility. *J. Comput. Chem.* **2009**, *30* (16), 2785−2791.

(20) Goodsell, D. S.; Olson, A. J. Automated docking of substrates to proteins by simulated annealing. *Proteins* **1990**, *8* (3), 195−202.

(21) Abraham, M. J.; Murtola, T.; Schulz, R.; Páll, S.; Smith, J. C.; Hess, B.; Lindahl, E. GROMACS: High performance molecular simulations through multi-level parallelism from laptops to super-computers. *SoftwareX* **2015**, *1*, 19−25.

(22) Best, R. B.; Zhu, X.; Shim, J.; Lopes, P. E.; Mittal, J.; Feig, M.; MacKerell, A. D., Jr. Optimization of the additive CHARMM all-atom protein force field targeting improved sampling of the backbone ϕ, ψ and side-chain $\chi1$ and $\chi2$ dihedral angles. *J. Chem. Theory Comput* **2012**, *8* (9), 3257−3273.

(23) Vanommeslaeghe, K.; Hatcher, E.; Acharya, C.; Kundu, S.; Zhong, S.; Shim, J.; Darian, E.; Guvench, O.; Lopes, P.; Vorobyov, I.; Mackerell, A. D. CHARMM general force field: A force field for drug-like molecules compatible with the CHARMM all-atom additive biological force fields. *J. Comput. Chem.* **2010**, *31* (4), 671−690.

(24) MacKerell, A. D.; Bashford, D.; Bellott, M.; Dunbrack, R. L.; Evanseck, J. D.; Field, M. J.; Fischer, S.; Gao, J.; Guo, H.; Ha, S.; Joseph-McCarthy, D.; Kuchnir, L.; Kuczera, K.; Lau, F. T. K.; Mattos, C.; Michnick, S.; Ngo, T.; Nguyen, D. T.; Prodhom, B.; Reiher, W. E.; Roux, B.; Schlenkrich, M.; Smith, J. C.; Stote, R.; Straub, J.; Watanabe, M.; Wiórkiewicz-Kuczera, J.; Yin, D.; Karplus, M. All-atom empirical potential for molecular modeling and dynamics studies of proteins. *J. Phys. Chem. B* **1998**, *102* (18), 3586−3616.

(25) Darden, T.; York, D.; Pedersen, L. Particle mesh Ewald: An N·log (N) method for Ewald sums in large systems. *J. Chem. Phys.* **1993**, *98* (12), 10089−10092.

(26) Páll, S.; Hess, B. A flexible algorithm for calculating pair interactions on SIMD architectures. *Comput. Phys. Commun.* **2013**, *184* (12), 2641−2650.

(27) Hurrle, S.; Hsu, W. H. The etiology of oxidative stress in insulin resistance. *Biomed J.* **2017**, *40* (5), 257−262.

(28) Agrawal, P. K. *Carbon-13 NMR of flavonoids*. Elsevier, 2019, 39, 41-49.

(29) Kumar, N. S.; Rajapaksha, M. Separation of catechin constituents from five tea cultivars using high-speed counter-current chromatography. *J. Chromatogr. A* **2005**, *1083* (1−2), 223−228.

(30) Spáčil, Z.; Nováková, L.; Solich, P. Comparison of positive and negative ion detection of tea catechins using tandem mass spectrometry and ultra high performance liquid chromatography. *Food Chem.* **2010**, *123* (2), 535−541.

(31) Panda, S.; Kar, A. Antidiabetic and antioxidative effects of *Annona squamosa* leaves are possibly mediated through quercetin-3-O-glucoside. *Biofactors* **2007**, *31* (3−4), 201−210.

(32) Tatsis, E. C.; Boeren, S.; Exarchou, V.; Troganis, A. N.; Vervoort, J.; Gerothanassis, I. P. Identification of the major constituents of *Hypericum perforatum* by LC/SPE/NMR and/or LC/MS. *Phytochemistry* **2007**, *68* (3), 383−393.

(33) Markham, K.; Ternai, B.; Stanley, R.; Geiger, H.; Mabry, T. Carbon-13 NMR studies of flavonoids—III: Naturally occurring flavonoid glycosides and their acylated derivatives. *Tetrahedron* **1978**, *34* (9), 1389−1397.

(34) Sudto, K.; Pornpakakul, S.; Wanichwecharungruang, S. An efficient method for the large scale isolation of naringin from pomelo (*Citrus grandis*) peel. *J. Food Sci. Technol.* **2009**, *44* (9), 1737−1742.

(35) Lallemand, J.; Duteil, M. 13C nmr spectra of quercetin and rutin. *Org. Magn. Reson* **1977**, *9* (3), 179−180.

(36) Pei, R.; Liu, X.; Bolling, B. Flavonoids and gut health. *Curr. Opin. Biotechnol* **2020**, *61*, 153−159.

(37) Sun, C.; Zhao, C.; Guven, E. C.; Paoli, P.; Simal-Gandara, J.; Ramkumar, K. M.; Wang, S.; Buleu, F.; Pah, A.; Turi, V.; Damian, G.; Dragan, S.; Tomas, M.; Khan, W.; Wang, M.; Delmas, D.; Portillo, M.

P.; Dar, P.; Chen, L.; Xiao, J. Dietary polyphenols as antidiabetic agents: Advances and opportunities. *Food Front.* **2020**, *1* (1), 18−44.

(38) Kousalya, P.; Jayanthy, V. Evaluation of phytochemicals and quantification of phenol, flavonoids and tannins of pods of *Leucaena leucocephala* (Lam.) De Wit. *Am. Eura. J. Agri. & Environ. Sci.* **2016**, *16* (9), 1561−1564. Deivasigamani, R. Phytochemical analysis of *Leucaena leucocephala* on various extracts. *J. Phytopharmacol* **2018**, *7* (6), 480−482.

(39) She, L.-C.; Liu, C.-M.; Chen, C.-T.; Li, H.-T.; Li, W.-J.; Chen, C.-Y. The anti-cancer and anti-metastasis effects of phytochemical constituents from *Leucaena leucocephala*. *Biomed Res.* **2017**, *28* (7), 2893−2897.

(40) Mohammed, R.; Souda, S.; Taie, H.; E.Moharam, M.; Shaker, K. Antioxidant, antimicrobial activities of flavonoids glycoside from *Leucaena leucocephala* leaves. *J. Appl. Pharm. Sci.* **2015**, *5* (6), 138−147.

(41) Chen, H.; Song, W.; Sun, K.-K.; Du, H.-W.; Wei, S.-D. Structure elucidation and evaluation of antioxidant and tyrosinase inhibitory effect and mechanism of proanthocyanidins from leaf and fruit of *Leucaena leucocephala*. *J. Wood Chem. Technol.* **2018**, *38* (6), 430−444.

(42) Kuppusamy, U. R.; Arumugam, B.; Azaman, N.; Jen Wai, C. *Leucaena leucocephala* fruit aqueous extract stimulates adipogenesis, lipolysis, and glucose uptake in primary rat adipocytes. *Sci. World* **2014**, *2014*, 737263 DOI: 10.1155/2014/737263.

(43) Kim, D. C.; In, M.-J. Antioxidative ability of ethanol extract from the leaves of *Leucaena leucocephala* (Lam.) de Wit. *J. Appl. Biol. Chem.* **2017**, *60* (2), 185−190.

(44) Renganathan, S.; Manokaran, S.; Vasanthakumar, P.; Singaravelu, U.; Kim, P.-S.; Kutzner, A.; Heese, K. Phytochemical profiling in conjunction with in vitro and in silico studies to identify human α-amylase inhibitors in *Leucaena leucocephala* (Lam.) De Wit for the treatment of diabetes mellitus. *ACS omega* **2021**, *6* (29), 19045−19057.

(45) Madayi, D.; Surya, P. H.; Elyas, K. K. A Glucose binding lectin from *Leucaena leucocephala* seeds and its mitogenic activity against human lymphocytes. *Int. J. Biol. Macromol.* **2020**, *163*, 431−441.

(46) Romero, N.; Areche, C.; Cubides-Cárdenas, J.; Escobar, N.; García-Beltrán, O.; Simirgiotis, M. J.; Céspedes, Á. In vitro anthelmintic evaluation of *Gliricidia sepium*, *Leucaena leucocephala*, and *Pithecellobium dulce*: Fingerprint analysis of extracts by UHPLC-orbitrap mass spectrometry. *Molecules* **2020**, *25* (13), 3002.

(47) Deghima, A.; Righi, N.; Rosales-Conrado, N.; León-González, M. E.; Baali, F.; Gómez-Mejía, E.; Madrid, Y.; Bedjou, F. Anti-inflammatory activity of ethyl acetate and *n*-butanol extracts from *Ranunculus macrophyllus* Desf. and their phenolic profile. *J. Ethno-pharmacol* **2021**, *265*, No. 113347.

(48) Bui, N. T.; Pham, T.-L. T.; Nguyen, K. T.; Le, P. H.; Kim, K.-H. Effect of extraction solvent on total phenol, flavonoid content, and antioxidant activity of *Avicennia officinalis*. *Res. Appl. Chem.* **2021**, *12*, 2678−2690.

(49) Nagle, D. G.; Ferreira, D.; Zhou, Y.-D. Epigallocatechin-3-gallate (EGCG): chemical and biomedical perspectives. *Phytochem-istry* **2006**, *67* (17), 1849−1855.

(50) Zhang, Z.; Li, Q.; Liang, J.; Dai, X.; Ding, Y.; Wang, J.; Li, Y. Epigallocatechin-3-O-gallate (EGCG) protects the insulin sensitivity in rat L6 muscle cells exposed to dexamethasone condition. *Phytomedicine* **2010**, *17* (1), 14−18.

(51) Wang, T.-y.; Li, Q.; Bi, K.-s. Bioactive flavonoids in medicinal plants: Structure, activity and biological fate. *Asian J. Pharm. Sci.* **2018**, *13* (1), 12−23.

(52) D'Andrea, G. Quercetin: a flavonol with multifaceted therapeutic applications? *Fitoterapia* **2015**, *106*, 256−271.

(53) Jayachandran, M.; Zhang, T.; Ganesan, K.; Xu, B.; Chung, S. S. M. Isoquercetin ameliorates hyperglycemia and regulates key enzymes of glucose metabolism via insulin signaling pathway in streptozotocin-induced diabetic rats. *Eur. J. Pharmacol.* **2018**, *829*, 112−120.

(54) Zhang, L.; Zhang, S.-T.; Yin, Y.-C.; Xing, S.; Li, W.-N.; Fu, X.-Q. Hypoglycemic effect and mechanism of isoquercitrin as an

inhibitor of dipeptidyl peptidase-4 in type 2 diabetic mice. *RSC adv* **2018**, *8* (27), 14967−14974.

(55) Naeem, A.; Ming, Y.; Pengyi, H.; Jie, K. Y.; Yali, L.; Haiyan, Z.; Shuai, X.; Wenjing, L.; Ling, W.; Xia, Z. M.; Shan, L. S.; Qin, Z. The fate of flavonoids after oral administration: A comprehensive overview of its bioavailability. *Crit. Rev. Food Sci. Nutr.* **2022**, *62* (22), 6169−6186.

(56) Terao, J. Potential role of quercetin glycosides as anti-atherosclerotic food-derived factors for human health. *Antioxidants* **2023**, *12* (2), 258.

(57) Jakaria, M.; Azam, S.; Jo, S.-H.; Kim, I.-S.; Dash, R.; Choi, D.-K. Potential therapeutic targets of quercetin and its derivatives: its role in the therapy of cognitive impairment. *J. Clin. Med.* **2019**, *8* (11), 1789.

(58) Kitada, M.; Ogura, Y.; Monno, I.; Koya, D. Sirtuins and type 2 diabetes: role in inflammation, oxidative stress, and mitochondrial function. *Front. Endocrinol.* **2019**, *10*, 187.

(59) Yoshizaki, T.; Milne, J. C.; Imamura, T.; Schenk, S.; Sonoda, N.; Babendure, J. L.; Lu, J.-C.; Smith, J. J.; Jirousek, M. R.; Olefsky, J. M. SIRT1 exerts anti-inflammatory effects and improves insulin sensitivity in adipocytes. *Mol. Cell. Biol.* **2009**, *29* (5), 1363−1374.

(60) Iside, C.; Scafuro, M.; Nebbioso, A.; Altucci, L. SIRT1 activation by natural phytochemicals: an overview. *Front. Pharmacol.* **2020**, *11*, 1225.

(61) Sarubbo, F.; Esteban, S.; Miralles, A.; Moranta, D. Effects of resveratrol and other polyphenols on Sirt1: relevance to brain function during aging. *Curr. Neuropharmacol.* **2018**, *16* (2), 126−136.